PHYSICS AND CHEMISTRY
OF SOLID STATE
V. 26, No.2 (2025) pp. 261-266

Section: Chemistry

DOI: 10.15330/pcss.26.2.261-266

Vasyl Stefanyk Precarpathian
National University

ФІЗИКА І ХІМІЯ ТВЕРДОГО ТІЛА
Т. 26, № 2 (2025) С. 261-266

Хімічні науки

UDC: 541.1.0:519.6:546

ISSN 1729-4428 (Print)
ISSN 2309-8589 (Online)

O. Vasiliev

First-principles study of mixing in the system of layered dichalcogenides MoS_2-WS_2

Frantsevich Institute for Problems of Materials Science National Academy of Sciences of Ukraine, o.vasiliev@ipms.kyiv.ua

The thermodynamic stability and mixing behavior of the MoS_2-WS_2 system were investigated using a cluster expansion model constructed from density functional theory (DFT) calculations. The alloy cluster expansion approach enabled the efficient sampling of atomic configurations, overcoming the computational limitations of direct DFT calculations. The accuracy of the cluster expansion model was validated against additional DFT calculations, achieving a root-mean-squared error close to $1.0 \cdot 10^{-4}$ eV/atom and R2 = 0.74. The mixing energy landscape was analyzed to determine the existence of ordered ground-state structures and assess the stability of solid solutions. The results indicate that MoS_2-WS_2 forms a stable solid solution across the full compositional range, with specific ordering tendencies at a broad range of intermediate atomic concentrations of tungsten, from XW = 0.33 to 0.66. The constructed convex hull suggests a multitude of ground states in this range with ordering patterns of a single solute atom residing in a hexagon of solvent atoms within a single layer. Generally small mixing energy values imply a dominant role of entropy at synthesis temperatures. The findings provide insight into the thermodynamic factors governing mixing in transition metal dichalcogenide MoS_2-WS_2 solid solutions, contributing to the rational design of materials based on them.

Keywords: transition metal dichalcogenides, solid solutions, mixing energy, ground states, Density Functional Theory, Alloy Cluster Expansion.

Received 16 February 2025; Accepted 01 June 2025.

Introduction

Layered Group 6 transition metal dichalcogenides represent a family of compounds of key importance for modern materials science. Due to their layered graphite-like structure, prominent electronic and optical properties, they have significant prospects of application in electronics [1–3], catalysis [4], energy harvesting [5] and storage [6] and other directions [7].

In recent years, increasing interest has been paid to the application of systems that contain more than one layered dichalcogenide. The efforts here are predominantly focused on the preparation and tuning of the properties of mixed materials by stacking layers of different dichalcogenides on top of each other or, in other words, creating nanoheterostructures (nanocomposites) based on them. Among the combinations under study, significant attention has been paid to such systems formed by the layers of molybdenum and tungsten disulfides [8], particularly for their prospects of application in optoelectronics and solar energy systems [9,10]. Authors of [11] concluded from their computational results that these dichalcogenides are the only among the studied that can form stable semiconducting layers, further underlining their importance for applications in electronics. The synthesis of these heterostructures usually implies strict process parameters control aimed at limiting the intermixing between the components kinetically. The methods are typically complex and multistage, such as dry transfer of individual layers [12,13], molecular beam epitaxy [14], stepwise chemical vapor deposition [15], and a number of wet methods either for stacking the layers from colloids or chemical reaction resulting in formation of one dichalcogenide layer on top of the other serving as a substrate (see [16] for a brief review of the wet methods). Of those, only the chemical vapor deposition and the wet approaches are suitable for scaling, and even there, the thermodynamics of mixing may play an important role. Solid solutions in the MoS_2-WS_2 system also attract attention by themselves, as promising for materials with tuned band gaps [1] and understanding the thermodynamics of mixing is crucial to devising and controlling their synthesis. Finally, the thermodynamics of mixing information is central in the assessment of the operational stability of these materials at conditions that allow the formation of equilibrium products, such as elevated temperatures that promote components diffusion.

Several theoretical studies were done previously to gain insight into the mixing energetics and behavior in the MoS_2-WS_2 system of solid solutions. In [17] the analysis was done using several representative structures calculated from the first principles, concluding on small overall mixing energy variation and no tendency for short-range ordering. Later cluster expansion modeling [1] suggested the existence of polymorphism region around the equimolar concentrations, but the authors offered no specifics about structural features of the possible ground states. Thus, a more focused look at the energies of mixing and their possible influence on its structure and stability would be of advantage.

This work aims to use the alloy cluster expansion method in conjunction with density functional theory calculations to assess the mixing behavior and elucidate structural specifics of the possible ground states in the MoS_2-WS_2 system.

I. Calculation details

All the first principles calculations for end members and mixed systems were done with density functional theory (DFT) and plane-wave basis of wavefunctions implemented in the PWscf code of the Quantum Espresso (QE) package [18]. Local density approximation (LDA) [19] was used as the exchange-correlation functional because of its good performance for 2H-MoS_2 [20] and 2H-WS_2 [21]. The files of pseudopotentials generated with the projector augmented wave (PAW) method were taken from the QE library. The kinetic energy cutoff of the basis plane waves assuring the total electron energy convergence within 1 meV/atom was 80 Ry. Integrations over the Brillouin zone were performed using grids of special points generated with the Monkhorst-Pack (MP) scheme [22] with the density that ensured the same total energy convergence. Because of the significant variation in size and shape of the calculated configurations, the Atomic Simulation Environment [23] *kspacing* method was used in practice with the maximum distance between k-points of 0.05 $Å^{-1}$. This setting corresponds to an 8×8×2 MP grid for the prototype unit cell of 2H-MoS_2. All initial structures were subject to structural optimization until the change in the total energy in two successive iterations did not exceed 10^{-4} eV. QE's default values were found suitable for other parameters involved in the calculations.

The mixing behaviour and its specifics were studied using the Alloy Cluster Expansion (CE) model [24] constructed from the DFT data. The CE construction and application, as well as most of the auxiliary operations, were done in Python programming language using the *icet* package [25]. The latter work provides an excellent description of the cluster expansion method and details of this particular realization, and they will not be reiterated here for the sake of space and focus. An important aspect to mention for this realization is the application of Machine Learning approaches to construct the models, allowing to work with underdetermined systems where the number of model parameters is higher than the number of configurations calculated with DFT and, thus, significant reduction of the computational resources needed to build the model. The specific tools from the package, as well as parameter values, are given in the Results and Discussion section.

II. Results and discussion

Alloy cluster expansion model construction

The main idea behind the cluster expansion is that by using a sufficiently large number of small structural configurations (training set) for which DFT calculations are feasible, a performant and computationally cheap model can be constructed (trained) that describes the target property for an arbitrarily large structural configuration with sufficient accuracy. The task is to find the balancing point between the size of the computational cost of preparing the training set, which directly correlates with its size, and the accuracy required to solve the problem at hand.

In this work, we took the following approach to prepare the training dataset. With the unit cell of 2H-MoS_2 as a prototype, we generated all the unique structural configurations in the system derived from it with the supercell sizes up to 4 unit cells and partial or complete replacement of Mo atoms with W, 333 configurations in total. Of those, all the configurations up to 3 unit cells and a subset of configurations with 4 unit cells, drawn in such a way that each available W concentration is represented at least by one of them, were selected for the training set and undergone a variable cell DFT structural optimization to calculate their total and mixing energies. The final training set contained 140 unique structural configurations in the MoS_2-WS_2 system.

The cutoffs for the pair, triplet, and quadruplet interactions to include in the model were determined by an exhaustive search using basic least squares as an underlying mechanism to approximate the expansion. The cutoffs were tested one by one for each type of interaction within 0.3 to 2.0 nm for pairs, 0.1 to 0.65 nm for triplets, and 0.1 to 0.7 nm for quadruplets with a step of 0.05 nm in each case. The lowest root mean squared error determined the best values within the tested ranges, and the final set of cutoffs were 1.65, 0.3, and 0.5 nm.

Of the algorithms of linear regression and feature selection available in the *icet* package, adaptive version of Least Absolute Shrinkage and Selection Operator (ad-LASSO) and Automatic Relevance Detection Regression (ARDR) demonstrated the lowest errors against the training set. Cluster expansions were built with both ARDR and ad-LASSO as the underlying linear models, and their performance was assessed by analyzing their predictions against the DFT mixing energies of the training set. To test the model's performance on larger systems, we also constructed and calculated with DFT three SQS supercells with sizes of 8 prototype unit cells and W atomic concentrations in the metal sub-lattice of 0.25, 0.5, and 0.75. ARDR demonstrated slightly better overall performance on the training set, especially for the structures at the upper and lower bounds of mixing energies (Fig. 1). More importantly, ARDR model predicted SQS mixing energies slightly better. While both models underestimate the energies, the errors with ARDR are lower at -21.0, -15.9, and -17.2% against -25.0, -14.5, and -22.0 with ad-LASSO, for the three quasi-random structures tested. Visual inspection of the deviations in Fig. 1 shows that SQS structures fall into a region in the middle of the mixing energy interval, where the model's performance is the poorest. Better quantitative predictions for the ground states are expected, as predictions near the convex hull lay within 1-5% deviations from the DFT data.

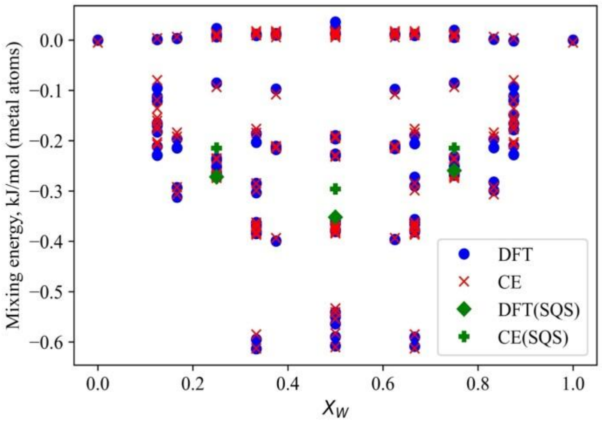

Fig. 1. Performance of the Cluster Expansion with ARDR as regression algorithm on training and SQS data.

The final Cluster Expansion model was built with the ARDR as an underlying linear regression and feature selection algorithm. The validation root-mean-squared error of the model was close to $1.0 \cdot 10^{-4}$ eV/atom of metal, suggesting that prediction, for the most part, was very close to the underlying DFT mixing energies. The R^2 score of 0.74 was achieved with the available data and selected model parameters, indicating that the model can give qualitative predictions with high confidence.

Of the initial 38 model parameters present in the model before training, only 18 retained non-zero values after the ARDR application, one representing the constant term in the cluster expansion and 17 others reflecting pair interactions between the atoms in the metal sub-lattice. The absence of the higher-order interactions directly follows from the cutoffs chosen by the mechanistic application of the search procedure, as described above. With the selected optimal cutoffs triplet and quadruplet clusters were not included in the model by construction. To check the impact of higher-order terms, the cutoffs for the third and fourth-order interactions were increased to 7.0 Å each, resulting in 10 triplets and 11 quadruplets in the expansion before training and feature selection. The algorithm selected none of the third-order interactions, but 7 quadruplets were deemed significant. On the other hand, their inclusion dropped the overall model performance in validation from R^2=0.74 to 0.55. The performance drop is obviously an outcome of insufficient sampling of the large enough configurations for the training set, as at least 4 unit cells are required to describe a quadruplet. The significant computational resources required to compute their DFT total energies limited the number of such structures. While the inclusion of such data is an apparent way to improve the model's accuracy, the R^2 score achieved with pair interactions only, in combination with very good local performance at the upper and lower bounds of the mixing energy, was considered a tradeoff sufficient for the purpose of this work.

Convex Hull

To get an in-depth insight into the mixing behavior in the system and assess the thermodynamic stability, as well as determine the structural specifics of the ground states, mixing energy was sampled on a large number of structural configurations, and a convex hull for the system was constructed. The structural sampling was done by constructing all possible unique configurations (structural enumeration) for the system sizes of 1 to 8 unit cells of the prototype with Mo atoms partially substituted by W. The enumerated set contained 98415 structural configurations, for which mixing energies were predicted using the cluster expansion model. The functionality for convex hull construction included in the *icet* package was then applied to these data.

Fig. 2 contains the plot of the data and the convex hull and suggests that, besides the end members, there are three defined ground states in the system at X_W=0.33, 0.5, and 0.66. On the other hand, at many concentrations where sampling is sufficient, there are structural configurations that lie in immediate proximity to the tie lines. Considering the tendency of the model to underestimate the mixing energy, especially in its middle section, it is safe to suggest that MoS_2-WS_2 solid solutions are thermodynamically stable in the whole concentration range.

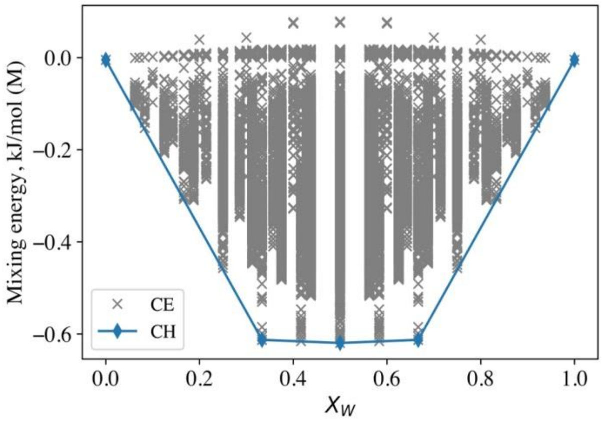

Fig. 2. Predicted mixing energies for unique structural configurations up to 4 prototype unit cells (CE) and the Convex Hull (CH)

A peculiar feature of the system, which is also present in [1], but not in [17], is the broad range of concentrations spanning from X_W = 0.33 to 0.66 with practically similar mixing energy for the ground states. In practice, it prevents any confident determination of the global ground

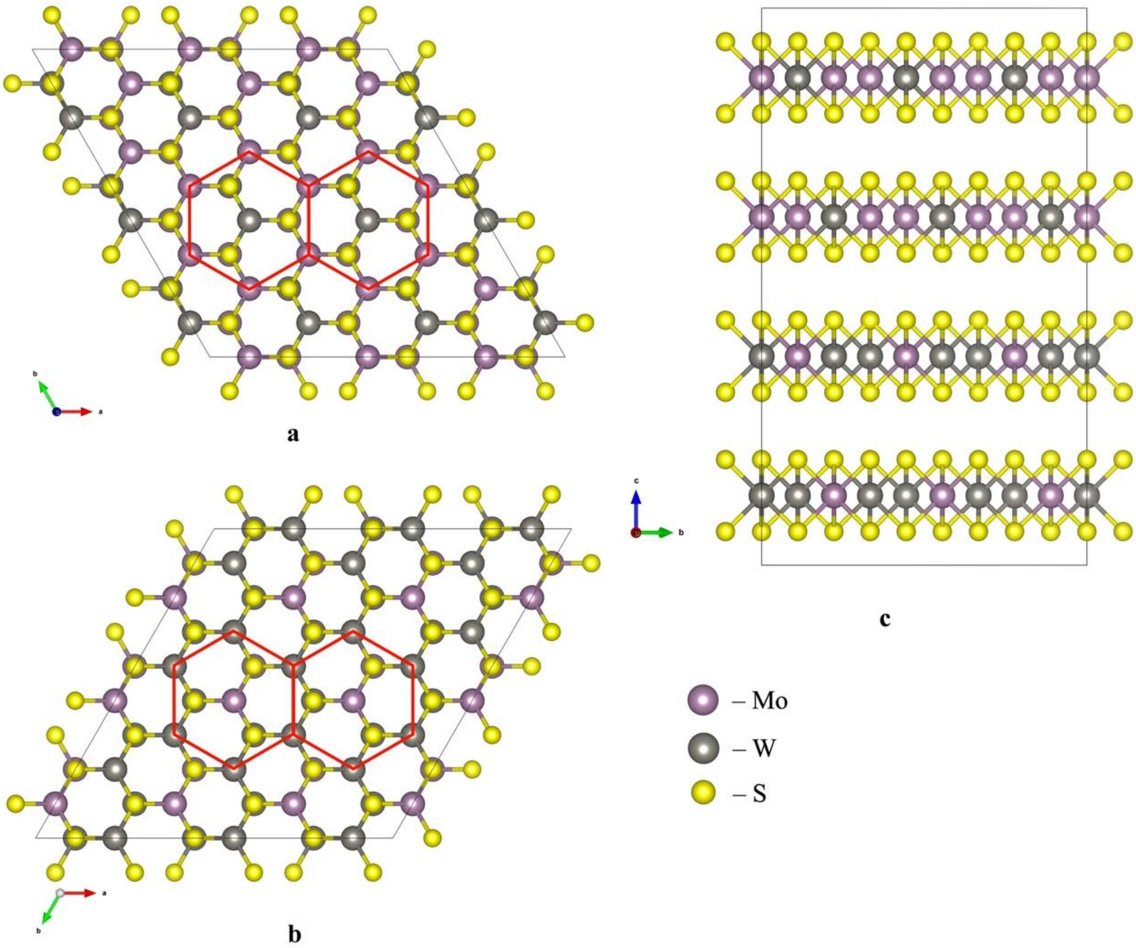

Fig. 3. Atomic structures of the equimolar ground state in the MoS_2-$MoSe_2$ system: top layer (a), bottom layer (b), lateral view (c).

state (lowest energy configuration for the system), and a series of structures (polymorphs) has to be considered for that role. On the other hand, such behavior may stem from specific ordering patterns, which might be important for the system's understanding. The ground states determined by the convex hull algorithm provide such an opportunity, representing the edges and the middle of this interval.

Atomic configuration of the equimolar ground state is given in Fig. 3 and shows that ordering in the system can, in principle, lead to the formation of an atomic pattern in which a hexagonal arrangement of the solvent atoms surrounds a solute atom within a single layer. For $X_W = 0.5$ the patterns alternate between the layers with several (two) Mo-rich layers followed by the same number of W-rich layers. For the ground state at $X_W = 0.33(3)$ the hexagons are formed by the Mo atoms and W atoms get entrapped inside them, similar to Fig. 3a, while for $X_W = 0.66(6)$ the situation is inverted and resembles the structure in Fig. 3b. All the intermediate ground states have their structures formed as a combination of this patterning.

Considering the differences in physical properties of Mo and W atoms, some local variation of electronic properties could be expected here, and achieving this patterning might be of interest in adsorption-related or other applications. On the other hand, the energy effects of such ordering are small and would be dominated by the entropy of mixing inputs at synthesis temperatures, which may prevent achieving the ordering in practice.

The following points can be drawn from a more general view of the mixing energy in the system as predicted by the CE. First, there are only a few configurations of the system with positive mixing energy, and even those can be artificial, considering the model accuracy. As the entropy of mixing will only improve the mixing at finite temperatures, the formation of solid solutions in the system is always thermodynamically favorable, which should be considered when devising the synthesis of materials in the system and designing their operational conditions. Second, the range of absolute values of the mixing energy in the system is rather small, within 0.7 kJ/mol of metal atoms. Thus, for most practical cases, entropic factors will determine the distribution of metal atoms within their sub-lattice, and the structure of the solid solution can be well represented as a random alloy of Mo and W atoms within a regular lattice of S atoms. On the other hand, the large number of polymorphic ground states provides a significant configurational space where the ordered patterning might be preserved despite entropic influences.

Conclusions

The results of sampling the cluster expansion model of the MoS_2-WS_2 system constructed with the first-principles training set demonstrate that the solid solutions are thermodynamically favorable in the whole concentration range with the negative mixing energy values for the dominant bulk of structural configurations. The deepest stabilization occurs in the broad range of concentrations spanning from $X_W = 0.33$ to 0.66 with a tendency to form atomic motifs where a single atom of one metal (Mo or W) is surrounded by a six-atom hexagon of the other metal. The absolute values of the mixing energy in the system are rather small, and at practical conditions, solid solution formation is expected to be dominated by the entropy of mixing while still preserving the possibility of structural patterning due to the polymorphic configurations.

The work was funded by the National Research Foundation of Ukraine under the project No. 2023.04/0046.

Vasiliev Oleksandr – PhD, Head of department of applied mathematics and computational experiment in materials science, Frantsevich Institute for Problems of Mterials Science NASU.

[1] A. Kutana, E.S. Penev, B.I. Yakobson, *Engineering electronic properties of layered transition-metal dichalcogenide compounds through alloying*, Nanoscale, 6, 5820 (2014); https://doi.org/10.1039/C4NR00177J.

[2] M. Ye, D. Zhang, Y.K. Yap, *Recent Advances in Electronic and Optoelectronic Devices Based on Two-Dimensional Transition Metal Dichalcogenides*, Electronics, 6, 43 (2017); https://doi.org/10.3390/electronics6020043.

[3] A. Piacentini, A. Daus, Z. Wang, M.C. Lemme, D. Neumaier, *Potential of Transition Metal Dichalcogenide Transistors for Flexible Electronics Applications*, Advanced Electronic Materials, 9, 2300181 (2023); https://doi.org/10.1002/aelm.202300181.

[4] D.M. Khaidar, W.N.R.W. Isahak, Z.A.C. Ramli, K.N. Ahmad, *Transition metal dichalcogenides-based catalysts for CO2 conversion: An updated review*, International Journal of Hydrogen Energy, 68, 35 (2024); https://doi.org/10.1016/j.ijhydene.2024.04.220.

[5] D.O. Idisi, B. Mwakikunga, *Two-dimensional layered metal dichalcogenides-based heterostructures for solar cells applications: A review*, Solar Energy, 263, 111981 (2023); https://doi.org/10.1016/j.solener.2023.111981.

[6] S. Ali, S.S. Ahmad Shah, M. Sufyan Javed, T. Najam, A. Parkash, S. Khan, M.A. Bajaber, S.M.M. Eldin, R.A. Tayeb, M.M. Rahman, J. Qi, *Recent Advances of Transition Metal Dichalcogenides-Based Materials for Energy Storage Devices, in View of Monovalent to Divalent Ions*, The Chemical Record, 24, e202300145 (2024); https://doi.org/10.1002/tcr.202300145.

[7] M. Samadi, N. Sarikhani, M. Zirak, H. Zhang, H.-L. Zhang, A.Z. Moshfegh, *Group 6 transition metal dichalcogenide nanomaterials: synthesis, applications and future perspectives*, Nanoscale Horizons, 3, 90 (2018); https://doi.org/10.1039/C7NH00137A.

[8] C. Chen, Y. Yang, X. Zhou, W. Xu, Q. Cui, J. Lu, H. Jing, D. Tian, C. Xu, T. Zhai, H. Xu, *Synthesis of Large-Area Uniform MoS2–WS2 Lateral Heterojunction Nanosheets for Photodetectors*, ACS Appl. Nano Mater., 4 5522 (2021); https://doi.org/10.1021/acsanm.1c00890.

[9] X. Hong, J. Kim, S.-F. Shi, Y. Zhang, C. Jin, Y. Sun, S. Tongay, J. Wu, Y. Zhang, F. Wang, *Ultrafast charge transfer in atomically thin MoS_2/WS_2 heterostructures*, Nat Nanotechnol., 9 682 (2014); https://doi.org/10.1038/nnano.2014.167.

[10] K. Chen, X. Wan, W. Xie, J. Wen, Z. Kang, X. Zeng, H. Chen, J. Xu, *Lateral Built-In Potential of Monolayer MoS2-WS2 In-Plane Heterostructures by a Shortcut Growth Strategy*, Adv. Mater., 27, 6431–6437 (2015); https://doi.org/10.1002/adma.201502375.

[11] C. Ataca, H. Şahin, S. Ciraci, *Stable, Single-Layer MX2 Transition-Metal Oxides and Dichalcogenides in a Honeycomb-Like Structure*, J. Phys. Chem. C, 116, 8983 (2012); https://doi.org/10.1021/jp212558p.

[12] M.A. Meitl, Z.T. Zhu, V. Kumar, K.J. Lee, X. Feng, Y.Y. Huang, I. Adesida, R.G. Nuzzo, J.A. *Rogers, Transfer printing by kinetic control of adhesion to an elastomeric stamp*, Nature Materials, 5 33 (2006); https://doi.org/10.1038/nmat1532.

[13] A. Castellanos-Gomez, M. Buscema, R. Molenaar, V. Singh, L. Janssen, H.S.J. van der Zant, G.A. Steele, *Deterministic transfer of two-dimensional materials by all-dry viscoelastic stamping*, 2D Mater., 1, 011002 (2014); https://doi.org/10.1088/2053-1583/1/1/011002.

[14] S. Vishwanath, X. Liu, S. Rouvimov, L. Basile, N. Lu, A. Azcatl, K. Magno, R.M. Wallace, M. Kim, J.-C. Idrobo, J.K. Furdyna, D. Jena, H.G. Xing, *Controllable growth of layered selenide and telluride heterostructures and superlattices using molecular beam epitaxy*, Journal of Materials Research, 31, 900 (2016); https://doi.org/10.1557/jmr.2015.374.

[15] Y. Gong, J. Lin, X. Wang, G. Shi, S. Lei, Z. Lin, X. Zou, G. Ye, R. Vajtai, B.I. Yakobson, H. Terrones, M. Terrones, B.K. Tay, J. Lou, S.T. Pantelides, Z. Liu, W. Zhou, P.M. Ajayan, *Vertical and in-plane heterostructures from WS2/MoS2 monolayers*, Nat Mater, 13, 1135 (2014); https://doi.org/10.1038/nmat4091.

[16] M. Morant-Giner, I. Brotons-Alcázar, N.Y. Shmelev, A.L. Gushchin, L.T. Norman, A.N. Khlobystov, A. Alberola, S. Tatay, J. Canet-Ferrer, A. Forment-Aliaga, E. Coronado, *WS2/MoS2 Heterostructures through Thermal Treatment of MoS2 Layers Electrostatically Functionalized with W3S4 Molecular Clusters*, Chemistry – A European Journal, 26, 6670 (2020); https://doi.org/10.1002/chem.202000248.

[17] H.-P. Komsa, A.V. Krasheninnikov, *Two-Dimensional Transition Metal Dichalcogenide Alloys: Stability and Electronic Properties*, J. Phys. Chem. Lett., 3 3652 (2012); https://doi.org/10.1021/jz301673x.

[18] P. Giannozzi, O. Andreussi, T. Brumme, O. Bunau, M. Buongiorno Nardelli, M. Calandra, R. Car, C. Cavazzoni, D. Ceresoli, M. Cococcioni, N. Colonna, I. Carnimeo, A. Dal Corso, S. de Gironcoli, P. Delugas, R.A. DiStasio, A. Ferretti, A. Floris, G. Fratesi, G. Fugallo, R. Gebauer, U. Gerstmann, F. Giustino, T. Gorni, J. Jia, M. Kawamura, H.-Y. Ko, A. Kokalj, E. Küçükbenli, M. Lazzeri, M. Marsili, N. Marzari, F. Mauri, N.L. Nguyen, H.-V. Nguyen, A. Otero-de-la-Roza, L. Paulatto, S. Poncé, D. Rocca, R. Sabatini, B. Santra, M. Schlipf, A.P. Seitsonen, A. Smogunov, I. Timrov, T. Thonhauser, P. Umari, N. Vast, X. Wu, S. Baroni, *Advanced capabilities for materials modelling with Quantum ESPRESSO*, J. Phys.: Condens. Matter, 29, 465901 (2017); https://doi.org/10.1088/1361-648X/aa8f79.

[19] J.P. Perdew, A. Zunger, *Self-interaction correction to density-functional approximations for many-electron systems*, Phys. Rev. B, 23, 5048 (1981); https://doi.org/10.1103/PhysRevB.23.5048.

[20] O.O. Vasiliev, *Thermodynamic Properties of Hexagonal Molybdenum Disulfide Calculated from First Principles*, Powder Metall. Met. Ceram., 58, 230 (2019); https://doi.org/10.1007/s11106-019-00068-x.

[21] O.O. Vasiliev, *Thermodynamic Properties of Tungsten Disulfide from First Principles in Quasi-Harmonic Approximation*, Powder Metall. Met. Ceram., 59 576 (2021); https://doi.org/10.1007/s11106-021-00185-6.

[22] H.J. Monkhorst, J.D. Pack, *Special points for Brillouin-zone integrations*, Phys. Rev. B, 13 5188 (1976); https://doi.org/10.1103/PhysRevB.13.5188.

[23] A. Hjorth Larsen, J. Jørgen Mortensen, J. Blomqvist, I.E. Castelli, R. Christensen, M. Dułak, J. Friis, M.N. Groves, B. Hammer, C. Hargus, E.D. Hermes, P.C. Jennings, P. Bjerre Jensen, J. Kermode, J.R. Kitchin, E. Leonhard Kolsbjerg, J. Kubal, K. Kaasbjerg, S. Lysgaard, J. Bergmann Maronsson, T. Maxson, T. Olsen, L. Pastewka, A. Peterson, C. Rostgaard, J. Schiøtz, O. Schütt, M. Strange, K.S. Thygesen, T. Vegge, L. Vilhelmsen, M. Walter, Z. Zeng, K.W. Jacobsen, *The atomic simulation environment—a Python library for working with atoms*, J. Phys.: Condens. Matter, 29, 273002 (2017); https://doi.org/10.1088/1361-648X/aa680e.

[24] J.M. Sanchez, *The Cluster Expansion Method*, in: J.L. Morán-López, J.M. Sanchez (Eds.), Theory and Applications of the Cluster Variation and Path Probability Methods (Springer US, Boston, MA,: 175 (1996); https://doi.org/10.1007/978-1-4613-0419-7_11.

[25] M. Angqvist, W.A. Muñoz, J.M. Rahm, E. Fransson, C. Durniak, P. Rozyczko, T.H. Rod, P. Erhart, *ICET – A Python Library for Constructing and Sampling Alloy Cluster Expansions*, Adv. Theory Simul., 2, 1900015 (2019); https://doi.org/10.1002/adts.201900015.

О. Васільєв

Змішування в системі шаруватих дихалькогенідів MoS_2-WS_2 з перших принципів

Інститут проблем матеріалознавства ім. І.М. Францевича Національної Академії Наук України, o.vasiliev@ipms.kyiv.ua

Термодинамічна стабільність і поведінка при змішуванні у системі MoS_2-WS_2 були досліджені за допомогою моделі кластерного розкладу, побудованої на основі розрахунків за теорією функціоналу електронної густини (DFT). Використання кластерного розкладу забезпечило ефективне залучення структурних конфігурацій для подолання обчислювальних обмежень прямих розрахунків за DFT. Модель кластерного розкладу була валідована додатковими розрахунками DFT та характеризувалась середньоквадратичною похибкою на рівні до $1{,}0 \cdot 10^{-4}$ еВ/атом і $R^2 = 0{,}74$. Ландшафт енергії змішування був проаналізований, щоб визначити існування впорядкованих структур основного стану та оцінити стабільність твердих розчинів. Результати показують, що MoS_2 та WS_2 утворюють стабільні тверді розчини у всьому діапазоні складу, зі специфічними тенденціями впорядкування в широкому діапазоні проміжних атомних концентрацій вольфраму, від $X_W = 0{,}33$ до $0{,}66$. Сконструйована опукла оболонка передбачає велику кількість основних станів у цьому діапазоні з мотивами впорядкування де один атом розчиненої речовини знаходиться в шестикутнику утвореному атомами розчинника у межах одного шару. В загальному малі значення енергії змішування вказують на домінуючу роль ентропії за температур синтезу. Отримані дані дають змогу зрозуміти термодинамічні чинники формування твердих розчинах дихалькогенідів перехідних металів системи MoS_2-WS_2, сприяючи раціональному дизайну матеріалів на їх основі.

Ключові слова: дихалькогеніди перехідних металів, тверді розчини, енергія змішування, основні стани, теорія функціоналу електронної густини, кластерний розклад сплавів.